Vibrational sidebands and dissipative tunneling in molecular transistors

Stephan Braig[1] and Karsten Flensberg[1,2]
[1]*Laboratory of Atomic and Solid State Physics, Cornell University, Ithaca, New York 14853, USA*
[2]*Ørsted Laboratory, Niels Bohr Institute fAPG, Universitetsparken 5, 2100 Copenhagen, Denmark*
(Received 12 March 2003; revised manuscript received 2 July 2003; published 24 November 2003)

Transport through molecular devices with strong coupling to a single vibrational mode is considered in the case where the vibration is damped by coupling to the environment. We focus on the weak tunneling limit, for which a rate equation approach is valid. The role of the environment can be characterized by a frictional damping term $\mathcal{S}(\omega)$ and a corresponding frequency shift. We consider a molecule that is attached to a substrate, leading to a frequency-dependent frictional damping of the single oscillator mode of the molecule, and compare it to a reference model with frequency-independent damping featuring a constant quality factor Q. For large values of Q, the transport is governed by tunneling between displaced oscillator states, giving rise to the well-known series of the Frank-Condon steps, while at small Q, there is a crossover to the classical regime with an energy gap given by the classical displacement energy. Using realistic values for the elastic properties of the substrate and the size of the molecule, we calculate I-V curves and find a qualitative agreement between our theory and recent experiments on C_{60} single-molecule devices.

DOI: 10.1103/PhysRevB.68.205324 PACS number(s): 73.23.Hk, 73.63.−b, 85.65.+h

I. INTRODUCTION

In the emerging field of single-molecule electronics there is a large interest in transport through mesoscopic systems with strong electron-phonon coupling. There has been a number of experiments in which transport through a single molecule has been reported.[1–6] One example is the series of experiments by Park *et al.*,[2] where it was shown that the current through a single C_{60} molecule was strongly coupled to a single vibrational mode. The single phonon mode was associated with the motion of the molecule in the confining potential created by the van der Waals interaction with the electrodes. Later, similar devices with more complicated molecules were investigated,[3,6] and they also showed excitation spectra which may be associated with emission of vibrational quanta.

Theoretically, there has been a large amount of work on the problem of tunneling through a single level with coupling to phonon modes. In many experimental realizations the tunnel coupling to the leads is rather weak, and the transport is dominated by the well-known Coulomb blockade effect. In this regime, where the transport is sequential, the use of a rate equation approach is appropriate rather than a coherent scattering approach. Motivated by the above mentioned single-molecule experiments, the rate equation approach has been used in a number of recent papers.[7–9] Some of these studies dealt with the issue of nonequilibrium phonon states, and the possibility of having negative differential conductance in such molecular systems.[7,8] Physically, it is an essential question how the excited vibrational levels are allowed to relax, either through coupling to the environment, for example, the phonons or plasmons of the metal substrate, or by virtue of the tunneling electrons.[10] In the case where the relaxation of the vibrational mode is faster than the tunneling rate one can assume an equilibrium phonon distribution.

The coupling between the vibrational mode and the environment depends strongly on which vibrational mode is considered. For intramolecular vibrations the lifetime can be very long.[11,12] However, for the experiments of Ref. 2, it was suggested that the vibrational motion was associated with a center of mass motion, which is coupled to the environment more strongly as we discuss in this paper. A sketch of the physical setup that we consider is shown in Fig. 1.

In this paper, we assume that the tunneling rate is much smaller than the rate of relaxation to other degrees of freedom. Hence, the usual rate equation approach is applicable, and we can assume that the phonons relax between each tunneling event according to a thermal boson distribution. We study a model of one single molecular orbital with strong Coulomb repulsion coupled to a dissipative environment. The dissipation is caused by coupling to phonon modes of the electrodes as well as electromagnetic modes and it is represented by a bath of harmonic oscillators. The description is thus similar to the well-known theory of Coulomb

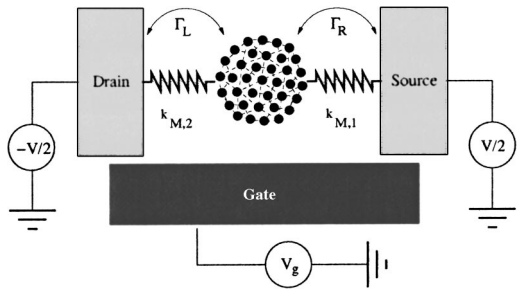

FIG. 1. Illustration of the system considered in this paper. The molecule is attached to substrates, e.g., by van der Waals interactions, and the movement in this potential is modeled by springs with spring constants $k_{M,1}$ and $k_{M,2}$. When an electron hops onto the molecule, the force created by image charges or local electric fields causes a shift of the equilibrium position of the oscillator and consequently emissions of quanta. The weights of the different final states are given by the well-known Frank-Condon overlap factors. The main objective of this paper is to consider the influence of damping of the molecular motion by emission of phonons into the substrates.

blockade in an electromagnetic environment.[13–16] However, there is a difference in how the coupling to the environment appears. In the electromagnetic environment case, the tunneling of an electron results in a sudden displacement of the position of the charge, while here the tunneling results in a sudden appearance of a force on the oscillator. For this reason, we go through the derivations in some detail and derive a general formula for the *I-V* curves. This general result does not depend on the nature of the environment but we then specialize to two cases. We consider a molecule attached to a substrate, using a continuum model for the substrate, and compare our result to a reference model featuring frequency-independent damping and quality factor. The *I-V* curves, as a function of the elastic parameters of the substrate and the size of the molecule, feature quite different line shapes as compared to the assumption of constant friction.

To get a simple estimate of the importance of the coupling to the substrate, consider a model where the molecule position x is coupled to a one-dimensional substrate through a spring with spring constant k_M. For small substrate displacements, force balance gives that

$$-k_M x \approx v_s^2 \rho_{1\mathrm{D}} \left(\frac{\partial u(z)}{\partial z} \right)_{z=0}, \tag{1}$$

where $u(z)$ is the substrate displacement, $\rho_{1\mathrm{D}}$ is the one-dimensional (1D) mass density, and v_s is the sound velocity. At a given frequency ω, the outgoing soundwaves are $u(z,\omega)=ae^{iz\omega/v_s}$, where a is a constant. Finding a from Eq. (1), we can insert it into the equation of motion for x to obtain the quality factor Q at the resonance frequency ω_0:

$$Q=\frac{m_0 \rho_{1\mathrm{D}} v_s \omega_0^3}{k_M^2}=\frac{\rho_{1\mathrm{D}} v_s}{m_0 \omega_0}=\frac{m}{m_0}, \tag{2}$$

where m_0 is the molecule mass with $\omega_0^2=k_M/m_0$, and $m=\rho_{1\mathrm{D}} v_s/\omega_0$ is the mass of a wavelength long piece of the substrate. With realistic parameters for a C_{60} molecule on a gold substrate, as was used in the experiments of Ref. 2, the quality factor is between 1 and 10, and therefore we expect the broadening to be substantial. This furthermore confirms the assumption that, for this type of molecular device, relaxation through the environment is much faster than through tunneling.

The paper is organized as follows. The model Hamiltonian is defined in Sec. II, and in Sec. III we derive an expression for the current from rate equations. The function that describes the tunneling density of states is then solved in the absence of the dissipative environment in Sec. IV and with coupling to the environment in Sec. V. We discuss different models for the dissipative coupling in Sec. VI, where we also discuss the physical implications. Section VII contains examples of *I-V* curves, and finally, a summary as well as a comparison with the experiments of Ref. 2 can be found in Sec. VIII.

II. MODEL HAMILTONIAN

We consider a model of one single spin-degenerate molecular level coupled to two leads (generalization to more molecular levels is straightforward). The single level is coupled to the vibrational mode of the molecule through the charge on the dot. The coupling between the oscillator and the environment is included as a linear coupling to a bath of harmonic oscillators in the spirit of the theory by Caldeira and Leggett.[17] The model Hamiltonian then reads

$$H=H_{LR}+H_D+H_B+H_{DB}+H_{\mathrm{bath}}+H_{B\mathrm{bath}}+H_T, \tag{3}$$

with

$$H_{LR}=\sum_{k\sigma,\ \alpha=L,R} \xi_{k\alpha} c_{k\sigma,\alpha}^\dagger c_{k\sigma,\alpha}, \tag{4a}$$

$$H_D=\sum_\sigma \xi_0 d_\sigma^\dagger d_\sigma + U n_{d\uparrow} n_{d\downarrow}, \tag{4b}$$

$$H_{\mathrm{B}}=\frac{p_0^2}{2m_0}+\frac{1}{2}m_0\omega_0^2 x_0^2, \tag{4c}$$

$$H_{DB}=\lambda x_0 \sum_\sigma d_\sigma^\dagger d_\sigma, \tag{4d}$$

$$H_{\mathrm{bath}}=\sum_j \left(\frac{p_j^2}{2m_j}+\frac{1}{2}m_j\omega_j^2 x_j^2 \right), \tag{4e}$$

$$H_{B\mathrm{bath}}=\sum_j \beta_j x_j x_0, \tag{4f}$$

where $c_{k\sigma,\alpha}^\dagger$, $c_{k\sigma,\alpha}$ and $d_\sigma^\dagger$, d_σ are the creation and annihilation operators for the leads and the dot, respectively, x_0 is the oscillator degree of freedom, $\{x_j\}$ describes the set of environment degrees of freedom and m_j and ω_j their respective masses and frequencies, ξ_0 is the on-site energy, and U is the Coulomb interaction on the molecule. The coupling constants for the electron-oscillator interaction and the oscillator-bath interaction are λ and $\{\beta_j\}$, respectively. The lead electron energies are given by

$$\xi_{k\alpha}=\varepsilon_{k\alpha}-\mu_\alpha, \tag{5}$$

where μ_α is the chemical potential of lead α. Finally, the tunnel Hamiltonian is

$$H_T=\sum_{k\sigma,\ \alpha=L,R} t_{k\alpha}(c_{k\sigma,\alpha}^\dagger d_\sigma + d_\sigma^\dagger c_{k\sigma,\alpha}). \tag{6}$$

The tunneling amplitudes could in principle also depend on the oscillator position. In the experimental realizations in Refs. 2–4, this is probably a small effect since the oscillator length is of the order of a few pm whereas the tunneling matrix element changes on the scale of nm. For simplicity, we do not take any such nonlinear effects into account, but we note that a position dependence of the tunneling amplitudes, for example of the form $\exp(-x_0/\ell_t)$, could easily be included in the present formalism.

The force acting on the charged molecule, represented by the term H_{DB}, is caused by electric fields originating from either static impurity charges or image charges. Since this force on the molecule is counteracted by a force on these charges and, hence, on the environment, we should in principle also include the interaction between the environment coordinates and the charge on the molecule. This would in fact lead to a qualitatively different behavior since Ohmic dissipation is cutoff at frequencies smaller than the inverse size of the total system, i.e., the inverse range of the interaction between the charge on the molecule and the charges in the environment. This interesting subtlety was pointed out in Ref. 18. However, since the van der Waals interaction between the molecule and substrate is short ranged compared to the electrostatic forces, we will consider the force acting on the molecule as an external quantity, which is thus not coupled to the dissipative environment. We do note, however, that including such a coupling would in fact lead to a small discontinuity at the beginning of each step in the *I-V* curve. The experimental data of, e.g., Ref. 2 do not seem to suggest such a discontinuity, and we therefore specialize to the case where the environment coordinates are unaffected by the charge on the molecule.

We now want to relate the coupling constants in the boson-bath coupling to the finite damping of the vibrational mode, which can be accomplished by studying the classical equations of motion. After removing the bath degrees of freedom, thereby neglecting the term H_{DB} that will be removed by a unitray transformation below, we end up with the following equation of motion in the frequency domain:

$$[\omega^2-\omega_0^2-\mathcal{S}(\omega)]x_0(\omega)=0, \tag{7}$$

where we have defined

$$\mathcal{S}(\omega)=\frac{1}{m_0}\sum_j \frac{\beta_j^2}{m_j}\frac{1}{(\omega+i\eta)^2-\omega_j^2}, \tag{8}$$

which is complex in general and gives rise to frictional damping and a frequency shift of the bare frequency ω_0. In Sec. VI B, we will explicitly calculate $\mathcal{S}(\omega)$ for the case of a molecule attached to a semi-infinite substrate.

We eliminate the coupling term H_{DB} of Hamiltonian (4) by a unitary transformation similar to the one used in the independent boson model,[19] at the cost of introducing displacement operators in the tunneling term. However, since we are dealing with a somewhat more complicated system due to the coupling to the bosonic bath, the unitary transformation in Ref. 19 has to be generalized. We define the transformation

$$\tilde{H}=SHS^\dagger, \quad S=e^{-iAn_d}, \quad A=p_0\ell+\sum_j p_j\ell_j, \tag{9}$$

where $n_d=\Sigma_\sigma d_\sigma^\dagger d_\sigma$. Using that

$$\tilde{x}_0=x_0-\ell n_d, \quad \tilde{x}_j=x_j-\ell_j n_d, \tag{10}$$

it is a matter of simple algebra to show that the linear coupling term H_{DB} cancels if we set

$$\ell=\frac{\lambda}{m_0[\omega_0^2+\mathcal{S}(0)]}, \quad \ell_j=\frac{-\ell\beta_j}{m_j\omega_j^2}, \tag{11}$$

and the Hamiltonian then transforms into

$$\tilde{H}=H_{LR}+\tilde{H}_D+H_B+H_{\rm bath}+H_{B\rm bath}+\tilde{H}_T, \tag{12}$$

where

$$\tilde{H}_T=\sum_{k\sigma,\ \alpha=L,R} t_{k\sigma,\alpha}(c_{k\sigma,\alpha}^\dagger e^{iA}d_\sigma+d_\sigma^\dagger e^{-iA}c_{k\sigma,\alpha}) \tag{13}$$

and

$$\tilde{H}_D=\varepsilon_0\sum_\sigma d_\sigma^\dagger d_\sigma+\tilde{U}n_{d\downarrow}n_{d\uparrow}, \quad \varepsilon_0=\xi_0-\frac{1}{2}\lambda\ell. \tag{14}$$

Here, $\tilde{U}=U-\lambda\ell$ is the Coulomb repulsion modified by the phonon mediated interaction. For a weak Coulomb interaction, this can result in a negative effective U, which was discussed in Ref. 20.

III. RATE EQUATIONS AND CURRENT FORMULA

We derive an expression for the current in the weak tunneling limit using the usual kinetic equation approach. As mentioned in Sec. I, the most important assumption here is that the tunneling rate is much smaller than all other time scales, which means that we can assume the vibrational degrees of freedom and the Fermi seas in the two electrodes to be in equilibrium at all times. For simplicity, we consider only two charge states and therefore let $U=\infty$, which leaves us with only three states: empty, and occupied by either spin up or down. The probabilities for the three states are denoted P_0, $P_\uparrow$, and $P_\downarrow$, respectively. The rate equations are

$$\begin{pmatrix} -2\Gamma_{10} & \Gamma_{01} & \Gamma_{01} \\ \Gamma_{10} & -\Gamma_{01} & 0 \\ \Gamma_{10} & 0 & -\Gamma_{01} \end{pmatrix}\begin{pmatrix} P_0 \\ P_\uparrow \\ P_\downarrow \end{pmatrix}=0, \tag{15}$$

which, combined with the condition $P_0+P_\downarrow+P_\downarrow=1$, has the solution

$$P_0=\frac{\Gamma_{01}}{\Gamma_{01}+2\Gamma_{10}}, \quad P_\downarrow=P_\uparrow=\frac{\Gamma_{10}}{\Gamma_{01}+2\Gamma_{10}}, \tag{16}$$

where Γ_{10} is the tunneling rate for tunneling from the empty state to a singly occupied state, and Γ_{01} is the rate for the reverse process. Since the electron can tunnel out of both left and right leads, both rates have left and right contributions: $\Gamma_{ij}=\Gamma_{ij}^L+\Gamma_{ij}^R$. The tunneling rates are calculated using Fermi's golden rule, thereby treating $\tilde{H}_T$ of Eq. (13) as the perturbation and assuming a thermal equilibrium distribution of the lead electrons and the phonon bath. Following standard derivations, we obtain

$$\Gamma_{10}^\alpha=\Gamma_\alpha\int\frac{d\omega}{2\pi}F(\omega)n_\alpha(\varepsilon_0+\omega), \tag{17a}$$

$$\Gamma_{01}^{\alpha}=\Gamma_{\alpha}\int\frac{d\omega}{2\pi}F(-\omega)[1-n_{\alpha}(\varepsilon_0+\omega)], \qquad (17b)$$

where we have defined the function

$$F(\omega)=\int_{-\infty}^{\infty}dt e^{i\omega t}F(t), \quad F(t)=\langle e^{iA(t)}e^{-iA}\rangle, \qquad (18)$$

in addition to the Fermi distributions of the two leads, $n_{\alpha}(\varepsilon)=(e^{\beta(\varepsilon-eV_{\alpha})}+1)^{-1}$, and the bare rates $\Gamma_{\alpha}=2\pi\Sigma_k|t_{k\alpha}|^2\delta(\xi_k)$. The function F has the properties

$$F(\omega)=F(-\omega)e^{\beta\omega}, \quad \int_{-\infty}^{\infty}\frac{d\omega}{2\pi}F(\omega)=1. \qquad (19)$$

We can use Eq. (19) to show that the rates in Eq. (17) can be written as

$$\Gamma_{10}^{\alpha}=\Gamma_{\alpha}\tilde{n}_{\alpha}, \quad \Gamma_{01}^{\alpha}=\Gamma_{10}^{\alpha}e^{\beta(\varepsilon_0-eV_{\alpha})}, \qquad (20)$$

where we defined

$$\tilde{n}_{\alpha}=\int\frac{d\omega}{2\pi}F(\omega)n_{\alpha}(\omega+\varepsilon_0). \qquad (21)$$

The current through the molecule is now given by

$$I=-e[2P_0\Gamma_{10}^{L}-(P_{\uparrow}+P_{\downarrow})\Gamma_{01}^{L}]=2e\frac{\Gamma_{10}^{R}\Gamma_{01}^{L}-\Gamma_{01}^{R}\Gamma_{10}^{L}}{\Gamma_{01}+2\Gamma_{10}}. \qquad (22)$$

Using Eq. (20), this can also be written as

$$I=\frac{2e\Gamma_L\Gamma_R\tilde{n}_R\tilde{n}_L(e^{\beta(\varepsilon_0-eV_L)}-e^{\beta(\varepsilon_0-eV_R)})}{\Gamma_L\tilde{n}_L(2+e^{\beta(\varepsilon_0-eV_L)})+\Gamma_R\tilde{n}_R(2+e^{\beta(\varepsilon_0-eV_R)})}. \qquad (23)$$

IV. WITHOUT COUPLING TO THE ENVIRONMENT

We start by discussing the limit when the oscillator is not coupled to the environment, which means that thermal smearing dominates over dissipative broadening. However, we still assume that the coupling is stronger than the tunnel coupling so that the molecule equilibrates between each tunneling event. This section is thus equivalent to the results in other rate equation calculations, but for completeness and later comparison we write down this limiting case.

The phonon average is performed assuming thermal equilibrium, and we have

$$F_0(t)=\langle e^{ip_0(t)\ell}e^{-ip_0(0)\ell}\rangle,$$

$$=\exp\{g(e^{-i\omega_0 t}-1)(1+N)+g(e^{i\omega_0 t}-1)N\}, \qquad (24)$$

where

$$g=\frac{1}{2}\left(\frac{\ell}{\ell_0}\right)^2, \quad \ell_0^2=\frac{1}{m_0\omega_0}, \quad N=n_B(\omega_0), \qquad (25)$$

Here, g is an important parameter determined by the ratio of the classical displacement length and the quantum mechanical oscillator length. The evaluation of $F_0(\omega)$ from Eq. (24) is equivalent to the independent boson model,[19] and using the result from there we get

$$F_0(\omega)=2\pi\sum_{n=-\infty}^{\infty}P_n(g)\,\delta(\omega-n\omega_0), \qquad (26)$$

where

$$P_n(g)=\exp[-g\coth(b)]e^{nb}I_n\left(\frac{g}{\sinh(b)}\right), \quad b=\frac{\beta\omega_0}{2}, \qquad (27)$$

and I_n is the modified Bessel function of the first kind. The finite-temperature result involves both positive and negative values of n, corresponding to the emission and absorption of phonons, respectively. At zero temperature, this reduces to having only positive values of n because of the factor $e^{n\beta\omega_0/2}$, and hence only emission processes are possible. In the limit $T\to 0$, we thus have a series of emission peaks at $\omega=n\omega_0$ for positive n and with weights given by the Poisson distribution $P_n\to e^{-g}g^n/n!$.

The current can now be found from Eq. (23). In Fig. 2, we show examples of current-voltage characteristics using Eq. (23) for symmetric and asymmetric junctions. In the following, we study how the physics gets modified by the coupling to the environment.

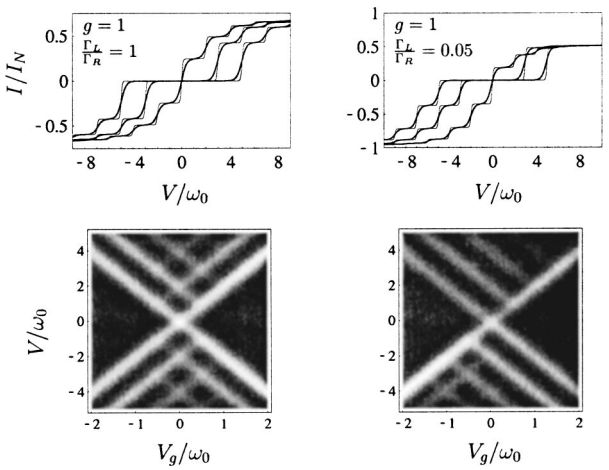

FIG. 2. Upper panels: current-voltage characteristics for a device without coupling to the environment for symmetric ($\Gamma_R=\Gamma_L$) and asymmetric ($\Gamma_R=0.05\Gamma_L$) tunneling contacts. Lower panels: contour plot of the differential conductance in the voltage-gate voltage plane, where $eV_g=\varepsilon_0$. The curves have been calculated using the analytic result Eq. (23), valid in the limit where the lifetime broadening of the oscillator is negligible. The temperature is $kT=0.1\omega_0$ for the thick lines and in the contour plots, while the thin lines are for $kT=0.025\omega_0$. The bias is applied symmetrically $V_L=V/2=-V_R$ and in the I-V curves we take ε_0 to be 0, 1.5, and 2.5 times ω_0. The current is measured in units of $I_N=e\Gamma_L\Gamma_R(\Gamma_L+\Gamma_R)$.

V. WITH COUPLING TO THE ENVIRONMENT

In presence of coupling to the environment, the evaluation of the function $F(t)$ in Eq. (18) is in principle straightfor-

ward since the Hamiltonian is quadratic in the oscillator and bath degrees of freedom. We obtain

$$F(t)=\exp[B(t)-B(0)], \quad B(t)=\langle A(t)A(0)\rangle_0, \quad (28)$$

where the operator A is defined in Eqs. (9) and (11). The expectation value $\langle\cdots\rangle_0$ is to be evaluated with respect to $\tilde{H}$ without the tunneling term. At this point, it is convenient to use the fluctuation-dissipation theorem,

$$B(\omega)=-2\,\mathrm{Im}[B^R(\omega)][1+n_B(\omega)], \quad (29)$$

to express $B(t)$ in terms of the corresponding retarded Green's function

$$B^R(t)=-i\theta(t)\langle[A(t),A(0)]\rangle_0. \quad (30)$$

Here, $n_B(\omega)=(e^{\beta\omega}-1)^{-1}$ is the usual Bose function. In order to find this retarded correlation function, we define the following auxiliary Green's functions:

$$G^R_{\mathcal{O}}(t)=-i\theta(t)\frac{1}{\ell}\langle[\mathcal{O}(t),A(0)]\rangle, \quad (31)$$

from which we obtain B^R as

$$B^R=\left(\ell G^R_{p_0}+\sum_j \ell_j G^R_{p_j}\right)\ell=\ell^2\left(G^R_{p_0}-\sum_j \frac{\beta_j}{m_j\omega_j^2}G^R_{p_j}\right). \quad (32)$$

The equations of motion for these functions are in frequency domain given by

$$\begin{pmatrix}\omega & -i/m_0\\ im_0\omega_0^2 & \omega\end{pmatrix}\begin{pmatrix}G^R_{x_0}\\ G^R_{p_0}\end{pmatrix}=\begin{pmatrix}i\\ 0\end{pmatrix}-\sum_j\begin{pmatrix}0\\ i\beta_j G^R_{x_j}\end{pmatrix}, \quad (33)$$

$$\begin{pmatrix}\omega+i\eta & -i/m_j\\ im_j\omega_j^2 & \omega+i\eta\end{pmatrix}\begin{pmatrix}G^R_{x_j}\\ G^R_{p_j}\end{pmatrix}=\begin{pmatrix}\frac{-i\beta_j}{m_j\omega_j^2}\\ 0\end{pmatrix}-\begin{pmatrix}0\\ i\beta_j G^R_{x_0}\end{pmatrix}. \quad (34)$$

Solving this linear set of equations for the Green's functions and inserting the results into Eq. (32), we obtain

$$B^R(\omega)=\frac{2g\bar{\omega}_0}{\omega^2-\bar{\omega}_0^2-\bar{\mathcal{S}}(\omega)}\left(1-\frac{\bar{\mathcal{S}}(\omega)}{\omega^2}\right), \quad (35)$$

where we have defined $\bar{\mathcal{S}}(\omega)\equiv\mathcal{S}(\omega)-\mathcal{S}(0)$ and the experimentally observable renormalized frequency $\bar{\omega}_0^2\equiv\omega_0^2+\mathcal{S}(0)$. Using Eq. (29), the function $B(\omega)$ thus follows as

$$B(\omega)=-4g\frac{1+n_B(\omega)}{\omega^2}\mathrm{Im}\left[\frac{\bar{\omega}_0^3}{\omega^2-\bar{\omega}_0^2-\bar{\mathcal{S}}(\omega)}\right], \quad (36)$$

where now $g=\ell^2/2\ell_0^2$ is defined with respect to the renormalized frequency $\bar{\omega}_0$, i.e., $\ell_0^2=1/m_0\bar{\omega}_0$. This result can then be used to find

$$F(t)=\exp\left(\int_{-\infty}^{\infty}\frac{d\omega}{2\pi}(e^{-i\omega t}-1)B(\omega)\right). \quad (37)$$

Equation (37) is equivalent to the result for the Coulomb blockade of a single tunnel junction with coupling to the electromagnetic environment.[14,15] In the Coulomb blockade problem, the tunneling density of states was related to the impedance as seen from the junction, here the I-V characteristic is in a similar way related to the frictional damping of the oscillator mode. In both cases, the low energy form of the spectrum is a power law at low temperatures. At small frequencies $\omega\ll\bar{\omega}_0$ and zero temperature, we get the following power law behavior:

$$F(\omega)\propto\omega^{\alpha-1}, \quad \alpha=\frac{2g}{\bar{\omega}_0\pi}\lim_{\omega\to 0}\left(\frac{\mathrm{Im}\,\bar{\mathcal{S}}(\omega)}{\omega}\right). \quad (38)$$

Furthermore, we use the trick by Minnhagen[21] to find the F function as the solution of the integral equation

$$F(\omega)=\frac{1}{\omega}\int_0^{\omega}\frac{d\zeta}{2\pi}F(\zeta)B(\zeta-\omega)(\zeta-\omega), \quad (39)$$

which is useful for the numerical evaluation of F.

VI. MODELS FOR $\mathcal{S}(\omega)$

A. Frequency-independent quality factor Q

As a first attempt, we can assume $\mathcal{S}$ to be of the form

$$\mathcal{S}(\omega)=\mathcal{S}(0)+i\frac{\omega\bar{\omega}_0}{Q}, \quad (40)$$

which leads to a frequency-independent quality factor Q of the single vibrational mode, similar to the Ohmic dissipation model of Caldeira and Leggett in Ref. 17. The model is also similar to the Coulomb blockade problem of an electric LCR circuit,[16] which is described by the same formula. The limit $Q\to\infty$ is seen to coincide with the results in Sec. IV, since in this limit $B(\omega)\to 2\pi(1+n_B(\omega))(\pm)\delta(\omega\pm\bar{\omega}_0)$, and when this is inserted into Eq. (37), we get Eq. (24). We also see that, for a critical value of $Q_c=2g/\pi$, the function F and, hence, the differential conductance change from having a divergence at small energies to vanish at small energies.

In Fig. 3, we plot the function F and its integral for different values of g and Q. It is clearly seen how the increasing dissipation smears the Frank-Condon steps. For strongly underdamped coupling to the environment, the steps are only weakly smeared, and still visible even for $Q=2.5$. For the special value of

$$Q=Q_c=\frac{2g}{\pi}, \quad (41)$$

the first step disappears and eventually for very small Q the function F goes towards a delta function, $F\to 2\pi\delta(\omega-g\bar{\omega}_0)$. Physically, this means that in the small Q limit, the system relaxes immediately to the classical state and tunneling is only possible by paying the total classical energy cost

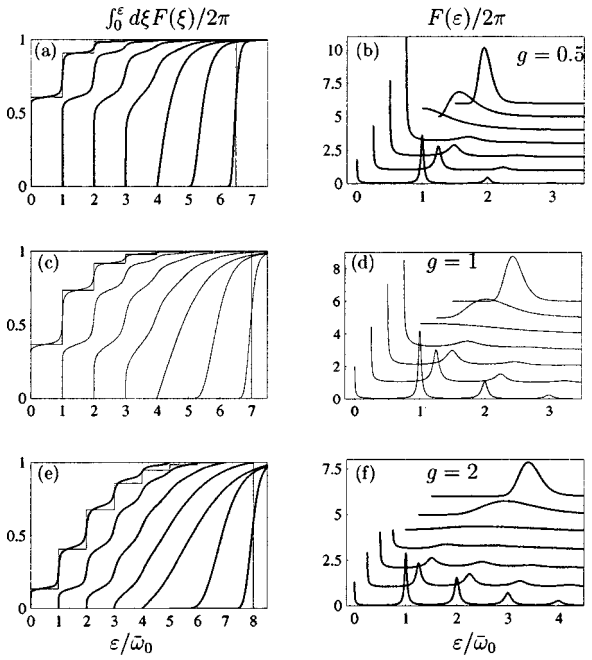

FIG. 3. The function $F(\xi)$ and its integral for different values of g and frequency-independent Q. The curves have been calculated from Eq. (39) at zero temperature. We take $Q=20,10,5,2.5,$ $2g/\pi,0.1,$ and 0.01, where $g=0.5$ in (a) and (b), $g=1$ in (c) and (d), and $g=2$ in (e) and (f). The curves have been displaced for clarity by multiples of (1,0) in (a), (c), and (e), and by multiples of (0.25,1) in (b), (d), and (f) (largest Q to the left). For large Q, the integrated function goes to the dissipationless results, where the step heights are given by the Poisson distribution [leftmost staircase in (a), (c), and (e)], whereas for small Q it goes to a step function at $\varepsilon=g\bar{\omega}_0$ (vertical line). Note also that the differential conductance at the first step remains sharp while the higher order steps are smeared when $Q>Q_c$.

of the displacement. To see this, we rewrite $g\bar{\omega}_0$ in terms of the coupling constant λ and get $\lambda\ell/2=\lambda^2/2m_0\bar{\omega}_0^2$, which is the classical energy for displacing the oscillator by increasing the occupation n_d by one.

The crossover to the classical regime occurs when the lifetime of the oscillator, $\bar{\omega}_0/Q$, is comparable to the Heisenberg uncertainty time associated with the classical energy of the displaced oscillator, i.e., when (reinserting $\hbar$)

$$\frac{Q_q}{\bar{\omega}_0}\equiv\frac{\hbar}{\lambda\ell/2}\Rightarrow Q_q=\frac{1}{g}. \tag{42}$$

The disappearance of the steps, which happens at Q_c, is therefore different from the crossover to the classical regime. This is shown in Fig. 4, where we plot the integral of F for $g=4$ for different values of Q. For $Q=20$, the steps are only slightly broadened, while for $Q=Q_c$, the steps are almost fully broadened but the line still follows the quantum behavior. Only for smaller Q do we approach the classical result, which is a step function at $g\bar{\omega}_0$.

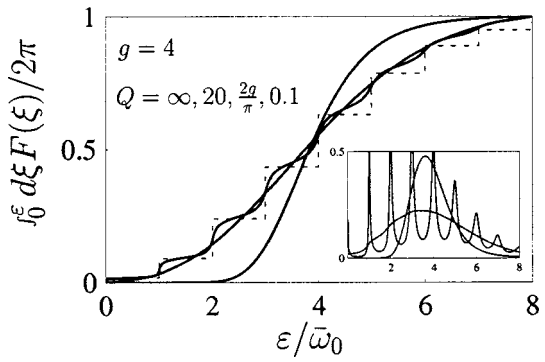

FIG. 4. The integral of the function F for $g=4$ and different Q at zero temperature. We take $Q=\infty$ (dashed line), 20, $8/\pi$, 0.1. At $Q\lesssim Q_c$ the steps disappear, while for $Q\lesssim Q_q$ the curves approach the classical limit, which is a step function at $\varepsilon=4\bar{\omega}_0$. The inset shows the F function itself for the same parameters.

B. Coupling to a substrate

We consider a molecule of mass m_0 attached to a substrate that extends over the semi-infinite half-space $z\geqslant 0$. The case of two substrates, as is shown in Fig. 1, is a straightforward generalization and will be discussed at the end of the calculation. The 3D Lagrangian density for the substrate is given by[22]

$$\mathcal{L}(\vec{r},t)=\frac{1}{2}\rho\Big[(\partial_t\vec{u})^2-(v_l^2-2v_t^2)(\vec{\nabla}\vec{u})^2-v_t^2(\vec{\nabla}\times\vec{u})^2 -2v_t^2\frac{\partial u_i}{\partial x_j}\frac{\partial u_j}{\partial x_i}\Big], \tag{43}$$

where v_l and v_t are the longitudinal and transverse sound velocities, and ρ is the mass density. This Lagrangian leads to the following equation of motion:

$$\partial_t^2\vec{u}-v_l^2\vec{\nabla}(\vec{\nabla}\vec{u})+v_t^2\vec{\nabla}\times\vec{\nabla}\times\vec{u}=0. \tag{44}$$

Having in mind a small molecule attached to the origin, the assumption of cylindrical symmetry around the z axis seems reasonable. We define u_r and u_z as the displacements in radial direction and parallel to the z axis, respectively.

We consider the case that the molecule only exerts a total force $\mathcal{F}$ perpendicular to the substrate surface:

$$\mathcal{F}=k_M\Big[x-\int_0^\infty 2\pi r f(r)u_z^0(r)dr\Big], \tag{45}$$

where $u_z^0(r)$ is the parallel displacement at the surface defined by $z=0$, and $f(r)$ is a normalized distribution function, i.e., $\int 2\pi r f(r)dr=1$. This imposes the following boundary conditions on the stress tensor T,[23]

$$T_{zr}|_{z=0}=0,\quad T_{zz}|_{z=0}=-\mathcal{F}f(r), \tag{46}$$

where the components T_{zr} and T_{zz} can be written as functions of the displacements u_r and u_z (see, e.g., Refs. 24 and 25). The solution is then a straightforward generalization of the procedure for a point source with $f(r)\propto\delta(r)/r$ outlined by Lamb in Ref. 26. We obtain, in frequency space,

$$u_z^0(r)=\mathcal{F}\frac{\omega^2}{v_t^2}\int_0^\infty \frac{k\nu_l f_k}{G(k,\omega)}J_0(kr)dk, \tag{47}$$

where we have defined the following quantities:

$$\nu_{t,l}=\begin{cases}\sqrt{k^2-\dfrac{\omega^2}{v_{t,l}^2}} & \text{if } k^2\geqslant\dfrac{\omega^2}{v_{t,l}^2},\\ -i\sqrt{k^2-\dfrac{\omega^2}{v_{t,l}^2}} & \text{if } k^2<\dfrac{\omega^2}{v_{t,l}^2},\end{cases} \tag{48}$$

$$G(k,\omega)=4\mu_L\nu_l\nu_t k^2-(\lambda_L+2\mu_L)(\nu_t^2+k^2)\nu_l^2+\lambda_L k^2\nu_t^2+\lambda_L k^4, \tag{49}$$

where μ_L and λ_L are the Lamé coefficients, which are related to the sound velocities as

$$v_l=\sqrt{\frac{\lambda_L+2\mu_L}{\rho}},\quad v_t=\sqrt{\frac{\mu_L}{\rho}}, \tag{50}$$

and f_k is the Fourier-Bessel transform of the force distribution $f(r)$,

$$f_k=\int_0^\infty f(r)J_0(kr)rdr. \tag{51}$$

The $(-)$ sign in the definition of $\nu_{t,l}$ in Eq. (48) is necessary for selecting the retarded response $\omega\rightarrow\omega+i\eta$ corresponding to outgoing waves since the square-root function has a branch cut on the negative real axis.

The total force $\mathcal{F}$ involves $u_z^0(r)$ and vice versa [see Eqs. (45) and (47)], so that we obtain

$$\int_0^\infty 2\pi r f(r)u_z^0(r)dr=x\frac{R(\omega)}{1+R(\omega)}, \tag{52}$$

where

$$R(\omega)=k_M\frac{2\pi\omega^2}{v_t^2}\int_0^\infty\frac{k\nu_l f_k^2}{G(k,\omega)}dk. \tag{53}$$

The function of interest, $\mathcal{S}(\omega)$, can then be deduced from the equation of motion for the molecule in frequency space:

$$-M\omega^2x_0(\omega)=-k_M\left[x_0(\omega)-\int_0^\infty 2\pi r f(r)u_z^0(r)dr\right]. \tag{54}$$

Identifying k_M/ω_M with the bare frequency ω_0^2, we obtain

$$\left[\omega^2-\omega_0^2+\omega_0^2\frac{R(\omega)}{1+R(\omega)}\right]x_0(\omega)=0, \tag{55}$$

which implies, upon comparison with Eq. (7),

$$\mathcal{S}(\omega)=-\omega_0^2\frac{R(\omega)}{1+R(\omega)}. \tag{56}$$

For the situation where the molecule is attached to two substrates it is simple to see that the function $\mathcal{S}(\omega)$ becomes instead

$$\mathcal{S}(\omega)=-\frac{k_{M,1}}{M}\frac{R_1(\omega)}{1+R_1(\omega)}-\frac{k_{M,2}}{M}\frac{R_2(\omega)}{1+R_2(\omega)}, \tag{57}$$

where $R_{1,2}$ is given by Eq. (53) but with k_M replaced by $k_{M1,2}$ and, if the two substrates are different, with substrate parameters changed accordingly. However, because of the lack of detailed knowledge about the actual geometry of the device, and since the coupling to the two sides of the junction is very likely to be asymmetric, we will make the simplifying assumption that the molecule only couples to one substrate.

Our results for $R(\omega)$ in Eq. (53) imply that the imaginary part of $\mathcal{S}(\omega)$ (which will eventually be responsible for the frictional damping) has contributions not only from extended waves in the substrate but also from waves that are confined to the surface, the so-called *Rayleigh* waves. Mathematically, this contribution arises from $G(k,\omega)$ being zero for a specific value of k. This value falls into the regime where both ν_t and ν_l are real, i.e., where wave vectors k are larger than allowed for transversal and longitudinal waves, see Eq. (48).[26]

In order to compare our result (56) to experimental data, we need to choose a specific model for the force distribution function $f(r)$. The most realistic model would involve a distribution in accord with the van-der-Waals potential, however, as a result of that f_k is a rather involved function of k. For simplicity, we therefore choose

$$f(r)=\frac{1}{2\pi D^2}e^{-r/D}\quad \text{i.e.,}\quad f_k=\frac{1}{2\pi\sqrt{1+k^2D^2}^3}. \tag{58}$$

The parameter D is on the order of the width D_0 of the molecule, e.g., $D_0=10.4$ Å for a C_{60} molecule. For this model, we can explicitly extract $\mathcal{S}(0)$, since then

$$R(0)=\frac{3}{64}\frac{\omega_0^2M\alpha^4}{(\alpha^2-1)\rho v_l^2D}, \tag{59}$$

where $\alpha\equiv v_l/v_t$. Note that $R(0)$ is proportional to the squared bare frequency $\omega_0^2=\bar{\omega}_0^2-\mathcal{S}(0)$ so that we end up with

$$\mathcal{S}(0)=-\bar{\omega}_0^2\frac{\bar{\omega}_0^2R(0)/\omega_0^2}{1+\bar{\omega}_0^2R(0)/\omega_0^2}. \tag{60}$$

This result has the particular effect on the damping coefficient $\mathrm{Im}\,\mathcal{S}(\omega)/\omega$ that it is independent of D/D_0 at zero frequency. We show plots of the real and imaginary parts of $\mathcal{S}(\omega)$ in Fig. 5. The real part, and thus the renormalization of the bare frequency as a function of energy, goes to zero rather quickly, whereas the imaginary part remains nonzero over a large frequency range. The latter is important for the damping since the quantity $\omega\bar{\omega}_0/\mathrm{Im}\,\mathcal{S}(\omega)$ takes the place of the quality factor. The fact that this quantity tends towards a

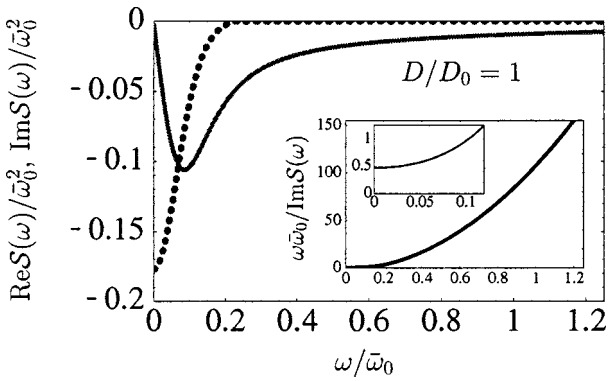

FIG. 5. Real part (dotted line) and imaginary part (solid line) of $\mathcal{S}(\omega)$ as a function of frequency for a C_{60} molecule on a gold substrate and the particular choice $D/D_0=1$. The imaginary part tends towards zero linearly, which is illustrated in the inset: the "quality factor" $\omega\bar{\omega}_0/\mathrm{Im}\,\mathcal{S}(\omega)$ tends towards a constant at zero frequency.

constant at zero frequency illustrates that the imaginary part of $\mathcal{S}(\omega)$ rises linearly with ω for small ω.

We plot the results for F and its integral in Fig. 6. First we note that the shape of the staircases is markedly different from the constant Q-factor model: they are asymmetric and less steep on the rising side with a rather sharp transition to the next step. The asymmetry is even more obvious in the peaks of F itself. We also note that a larger spread of the coupling over the surface, i.e., larger D/D_0, makes the peaks in F and the steps in its integral sharper and less asymmetric. For large D/D_0, the staircase tends towards the large constant Q limit of before, since then $\omega/\mathrm{Im}\,\mathcal{S}(\omega)$ grows rapidly with ω and at the same time $\mathcal{S}(0)\to 0$.

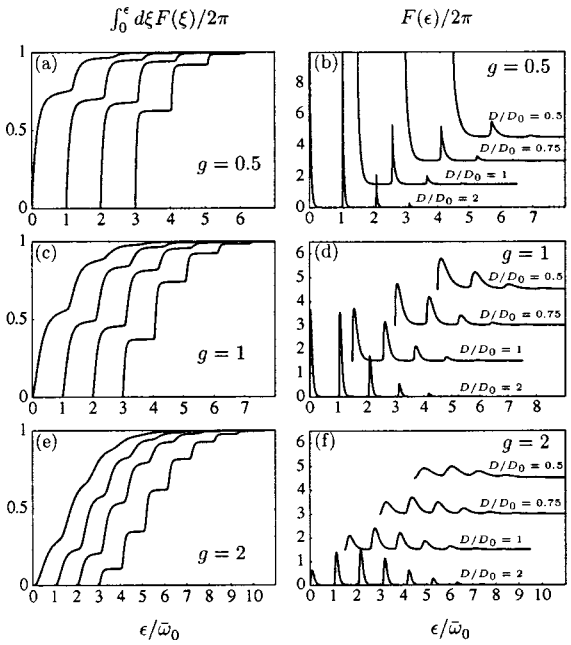

FIG. 6. The function $F(\xi)$ and its integral for different values of g, making use of (56) for $\mathcal{S}(\omega)$. The curves have been calculated from Eq. (39) at zero temperature, assuming a C_{60} molecule attached to a gold substrate. We take $D/D_0=0.5$, 0.75, 1, and 2, where $g=0.5$ in (a) and (b), $g=1$ in (c) and (d), and $g=2$ in (e) and (f). The curves have been displaced for clarity by multiples of (1,0) in (a), (c), and (e) (largest D/D_0 to the right), and by multiples of (1.5,1.5) in (b), (d), and (f) (largest D/D_0 at the bottom). The staircases in (a), (c), and (e) feature sharper and less asymmetric steps for larger D/D_0 but are clearly visible in any case. The asymmetry is even more apparent in the plots of F in (b), (d), and (f). In contrast to the constant Q-factor results in Fig. 3, even the first step in the staircase gets smeared for smaller D/D_0. However, we recover the large constant-Q limit for large D/D_0.

VII. *I-V* CURVES

In this section, we show a number of I-V curves using the expression in Eq. (23) at zero temperature based on the F function, both for the case of frequency-independent quality factor and for the substrate model (56) for $\mathcal{S}(\omega)$ discussed in Sec. VI. In Fig. 7, we show current-voltage characteristics for constant $Q=5$ and $g=0.5$, 1, and 2. For this value of Q, the Frank-Condon steps are still visible. If we took even smaller values of Q (not shown) such that the steps disappear, the characteristics are still strongly modified by the electron-vibron coupling in the sense that a gap develops in the I-V curve. Such an effect was recently claimed to be observed in a different type of device.[27]

We also show I-V curves corresponding to a C_{60} molecule coupled to a gold substrate, using the substrate model of Sec. VI B; see Fig. 8. We display the I-V curves for $g=0.5$, 1, and 2, both for symmetric and for asymmetric tunneling contacts, however, we restrict ourselves to $D/D_0=1$ since the general features are very similar for other choices of D/D_0. Upon comparison with the frequency-independent Q-factor model, we note that the I-V staircases are in general less steep and smoother but still clearly exhibit the expected Frank-Condon steps.

VIII. SUMMARY AND DISCUSSION

A. Summary

We have included broadening of the phonon sidebands due to frictional coupling of the oscillator mode within a kinetic equation approach. Since we have worked in the limit where the tunneling time is much smaller than the lifetime of the oscillator, we have assumed that the oscillator and the environment are in thermal equilibrium and in this case an analytical result for the current is obtained.

In the reference model featuring the frequency independent oscillator quality factor Q, we recover the usual Frank-Condon physics for large values of Q. The transition between the two different charge states is then given by the usual overlap of two displaced oscillator wavefunctions, the governing parameter being the ratio of the displacement length ℓ and the oscillator length ℓ_0, or $g=\ell^2/2\ell_0^2$. For moderate quality factors $Q>Q_c=2g/\pi$, the steps are smeared but still visible. For even smaller values of the quality factor, the decay time of the oscillations becomes shorter than the quantum mechanical uncertainty time, which happens when Q

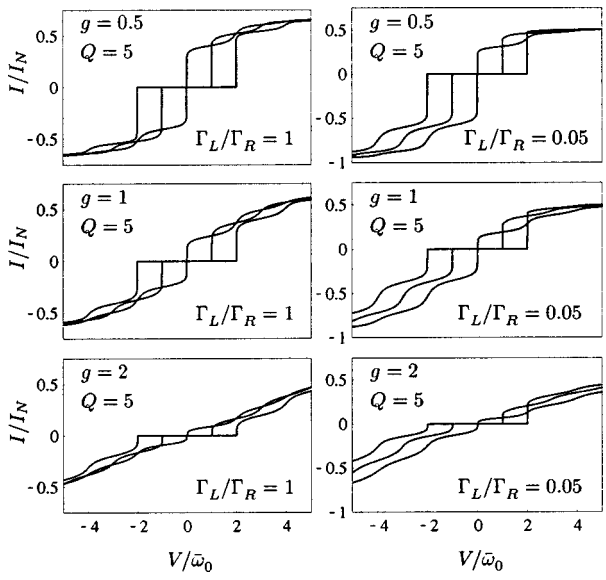

FIG. 7. Current-voltage characteristics for $g=0.5$, 1, and 2, and frequency-independent $Q=5$ at zero temperature. In each panel, we have taken $\varepsilon_0=0$, $0.5\bar{\omega}_0$, and $\bar{\omega}_0$, and the voltage is applied symmetrically across the device, so that $V_L=V/2=-V_R$. The current is measured in units of $I_N=e\Gamma_L\Gamma_R(\Gamma_L+\Gamma_R)$. The panels on the left show the case of symmetric tunneling contacts, whereas the panels on the right side correspond to asymmetric tunneling contacts with $\Gamma_L/\Gamma_R=0.05$.

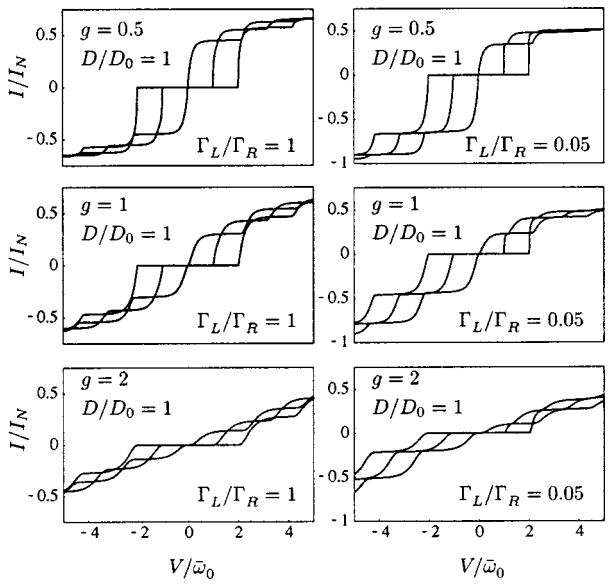

FIG. 8. Current-voltage characteristics for $g=0.5$, 1, and 2 using Eq. (56) for $\mathcal{S}(\omega)$ at zero temperature, calculated for a C_{60} molecule on gold. In each panel, we have taken $\varepsilon_0=0$, $0.5\bar{\omega}_0$, and $\bar{\omega}_0$, and the voltage is applied symmetrically across the device, so that $V_L=V/2=-V_R$. The current is measured in units of $I_N=e\Gamma_L\Gamma_R(\Gamma_L+\Gamma_R)$. The panels on the left show the case of symmetric tunneling contacts, whereas the panels on the right side correspond to asymmetric tunneling contacts with $\Gamma_L/\Gamma_R=0.05$.

$<1/g$. In this strongly damped case the tunneling process crosses over to a regime with a gap given by the classical displacement energy.

We were also able to calculate $\mathcal{S}(\omega)$ for a molecule that is attached to a substrate and showed how the molecule loses energy to the substrate. The model features similar general results to the constant Q-factor model, however, it is different in that the steps in the I-V curves rise more smoothly but feature a rather sharp transition to the next step, which then again rises up smoothly. The underlying reason for this is the peak structure of F, which exhibits asymmetric peaks due to the frequency dependent damping coefficient. We also note the dependence on the spread of the coupling over the substrate surface, parametrized by D/D_0, where our results tend towards the large constant Q limit for large D/D_0.

B. Comparison with experiments

We have also tried to fit the present theoretical results to the experiments in Ref. 2, for which the theory should be appropriate since the tunneling broadening is much smaller than the temperature, oscillator quantum, and observed widths. For these experiments, in which C_{60} molecules were attached to two leads, it therefore seems likely that the broadening is dominated by coupling to the environment.

A rough qualitative agreement, except for the steepness on the rising side of the steps, can be achieved for the frequency-independent quality factor if we assume $g\approx 1-2$ and $Q\approx 2-6$. However, in order to obtain quantitative agreement, it is necessary to assume different values for g and Q for different values of the gate and source-drain voltages.

Our model for $\mathcal{S}(\omega)$ that corresponds to a molecule attached to a substrate (see Sec. VI B) features qualitative agreement with experiment if we assume g and D/D_0 to be on the order of unity. The asymmetry in the peak structure of F actually provides for a better quantitative fit to the experimental data than is possible for the constant Q-factor model. This is illustrated in Fig. 9.

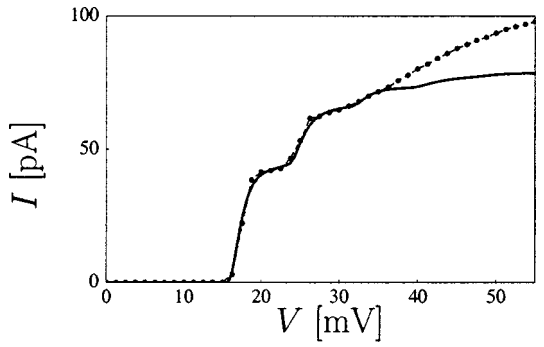

FIG. 9. Example of a fit to the experimental curves of Ref. 2 using the substrate model (56) for a C_{60} molecule on gold, with $g=2$ and $D/D_0=0.75$. The dots are experimental data points for a gate voltage of 6.8 V and positive bias voltage, and the solid line is the theoretical curve. The smearing of the first step is seen to be reproduced well, while at the same time showing a sharp rise for the second step. This kind of smearing could not be produced by thermal smearing, which would smear both steps equally. However, it is not possible to make consistent fits for the entire I-V curve and for different gate voltages. This suggests that the molecule might be changing position and/or coupling with changing voltages.

ACKNOWLEDGMENTS

The authors acknowledge discussions with P. Brouwer, A.-P. Jauho, P. McEuen, T. Novotny, J. Park, and J. Sethna. The work was supported by the Cornell Center for Materials Research under NSF Grant No. DMR0079992, by the Danish National Research Council, and by the Packard Foundation.

[1] M.A. Reed, C. Zhou, C.J. Muller, T.P. Burgin, and J.M. Tour, Science **278**, 252 (1997).
[2] H. Park, J. Park, A.K.L. Lim, E.H. Anderson, A.P. Alivisatos, and P.L. McEuen, Nature (London) **407**, 57 (2000).
[3] J. Park, A.N. Pasupathy, J.I. Goldsmith, C. Chang, Y. Yaish, J.R. Petta, M. Rinkoski, J.P. Sethna, H.D. Abruna, P.L. McEuen, and D.C. Ralph, Nature (London) **417**, 722 (2002).
[4] W. Liang, M.P. Shores, M. Bockrath, J.R. Long, and H. Park, Nature (London) **417**, 725 (2002).
[5] R.H.M. Smit, Y. Noat, C. Untiedt, N.D. Lang, M.C. van Hemert, and J.M. van Ruitenbeek, Nature (London) **419**, 906 (2002).
[6] N.B. Zhitenev, H. Meng, and Z. Bao, Phys. Rev. Lett. **88**, 226801 (2002).
[7] D. Boese and H. Schoeller, Europhys. Lett. **54**, 668 (2001).
[8] K. McCarthy, N. Prokof'ev, and M. Tuominen, Phys. Rev. B **67**, 245415 (2003).
[9] A. Mitra, I. Aleiner, and A.J. Millis, cond-mat/0302132 (unpublished).
[10] V. Aji, J. Moore, and C. Varma, cond-mat/0302222 (unpublished).
[11] V.L. Gurevich and H.R. Schober, Phys. Rev. B **57**, 11295 (1998).
[12] K.R. Patton and M.R. Geller, Phys. Rev. B **67**, 155418 (2003).
[13] Y.V. Nazarov, Zh. Éksp. Teor. Fiz. **95**, 975 (1989) [Sov. Phys. JETP **68**, 561 (1989)].
[14] M.H. Devoret *et al.*, Phys. Rev. Lett. **64**, 1824 (1990).
[15] S.M. Girvin *et al.*, Phys. Rev. Lett. **64**, 3183 (1990).
[16] G.-L. Ingold and H. Grabert, Europhys. Lett. **14**, 371 (1991).
[17] A.O. Caldeira and A.J. Leggett, Ann. Phys. (N.Y.) **149**, 374 (1983).
[18] A.A. Louis and J.P. Sethna, Phys. Rev. Lett. **74**, 1363 (1995).
[19] G. D. Mahan, *Many-Particle Physics* (Plenum Press, New York, 1990).
[20] A. Alexandrov and A. Bratkovsky, Phys. Rev. B **67**, 235312 (2003).
[21] P. Minnhagen, Phys. Lett. **56A**, 327 (1976).
[22] H. Ezawa, Ann. Phys. (N.Y.) **67**, 438 (1971).
[23] The stress tensor is defined as $d\vec{F}=Td\vec{A}$, where $d\vec{F}$ is an infinitesimal force, and $d\vec{A}$ is an infinitesimal area element.
[24] L. D. Landau and E. M. Lifshitz, *Theory of Elasticity* (Pergamon Press, New York, 1959).
[25] W. M. Ewing, W. S. Jardetzky, and F. Press, *Elastic Waves in Layered Media* (McGraw-Hill, New York, 1957).
[26] H. Lamb, Philos. Trans. R., Soc. London, Ser. A **203**, 1 (1904).
[27] E.M. Höhberger *et al.*, cond-mat/0304136 (unpublished).